

## Research Article

# Trajectory Tracking Control for WMRs with the Time-Varying Longitudinal Slippage Based on a New Adaptive SMC Method

Zhi Li<sup>1</sup>, Bo You,<sup>1</sup> Liang Ding<sup>2</sup>, Haibo Gao<sup>2</sup>, and Fengxiang Huang<sup>3</sup>

<sup>1</sup>Mechanical & Power Engineering College, Harbin University of Science and Technology, Harbin, China

<sup>2</sup>State Key Laboratory of Robotics and System, Harbin Institute of Technology, Harbin, China

<sup>3</sup>Networking BU, TP-Link Technology, Shenzhen, China

Correspondence should be addressed to Liang Ding; liangding@hit.edu.cn

Received 1 March 2019; Revised 28 June 2019; Accepted 16 July 2019; Published 20 August 2019

Academic Editor: Paolo Castaldi

Copyright © 2019 Zhi Li et al. This is an open access article distributed under the Creative Commons Attribution License, which permits unrestricted use, distribution, and reproduction in any medium, provided the original work is properly cited.

Wheeled mobile robots (WMRs) in real complex environments such as on extraterrestrial planets are confronted with uncertain external disturbances and strong coupling of wheel-ground interactions while tracking commanded trajectories. Methods based on sliding mode control (SMC) are popular approaches for these situations. Traditional SMC has some potential problems, such as slow convergence, poor robustness, and excessive output chattering. In this paper, a kinematic-based feed-forward control model is designed for WMRs with longitudinal slippage and applied to the closed-loop control system for active compensation of time-varying slip rates. And a new adaptive SMC method is proposed to guide a WMR in trajectory tracking missions based on the kinematic model of a general WMR. This method combines the adaptive control method and a fast double-power reaching law with the SMC method. A complete control loop with active slip compensation and adaptive SMC is thus established. Simulation results show that the proposed method can greatly suppress chattering and improve the robustness of trajectory tracking. The feasibility of the proposed method in the real world is demonstrated by experiments with a skid-steered WMR on the loose-soil terrain.

## 1. Introduction

Wheeled mobile robots (WMRs) have been widely utilized for exploration tasks on both earth and extraterrestrial bodies. Many current researchers make assumptions that the wheels and the ground have no relative slip or skidding, to simplify the description and analysis of the external uncertainty. However, when WMRs locomote on soft or rugged terrain, which is a nonholonomic constraint system as in [1, 2], control laws developed with the ideal assumptions may not ensure a decent real-time performance of tracking trajectories.

Some researchers performed a series of studies on the dynamic interaction between WMRs' wheels and unstructured terrain [3–5]. They intended to reveal the mechanism of the occurrence of slippage and skid, and thus, the control model can be theoretically accurate. But due to the complexity of a dynamic integral model and the difficulty of making necessary measurements, these mechanism-based control laws have been difficult to be directly applied to real WMRs

so far. On the other hand, kinematic models are relatively concise and easy to establish. They are often utilized with different control laws [6, 7] for real-time applications. However, these methods usually treat the uncertainty of WMRs on soft or rugged terrains as external interferences, which greatly decrease their robustness in real environments.

The capability of WMR tracking trajectories can be viewed as a nonlinear question which is strongly coupled with real environments and WMR models. Sliding mode control (SMC) is a popular approach for trajectory tracking under these circumstances. The reaching law generally has a significant effect on the performance of the entire SMC loop. The constant reaching law [8] is easy to implement but has a low convergence rate. An exponential reaching law [9] can converge quickly but suffers from obvious chattering when approaching the sliding surface. The power reaching law [10] can be relatively steady around the sliding surface, but its convergence is slow when the state of the system is far from the steady-state surface. Therefore, some

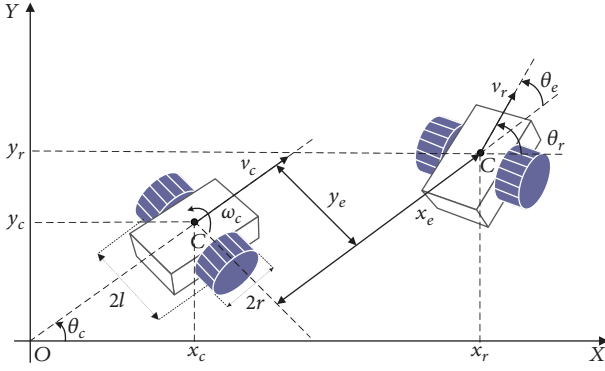


FIGURE 1: Wheeled mobile robot pose error.

researchers have endeavored to balance these characteristics to find solutions for practical problems. Matraji et al. [7] applied the double-power reaching law to solve the control problem for the descending stage for a soft landing on an asteroid. Gu et al. [11] designed a double-power reaching rate for near space vehicle control, which guarantees good dynamic characteristics of the trajectory tracking.

Although the methods mentioned above have some positive characteristics in certain circumstances, they still lack the ability to suppress output chattering. This can cause unpredictable results for robots' motion in complex environments. Therefore, adaptive control is necessary for the situations when the task requirements put a high priority on stability. Liu et al. [12] applied fuzzy wavelet neural networks to SMC for robot manipulators, achieving a better performance by compensating for the estimated uncertainty. Yen et al. [13] proposed an adaptive fast double-power approach for motion tracking of a two dimensional table servo system. Wang et al. [14] proposed an adaptive second-order SMC approach for the trajectory tracking of a skid-steered WMR to overcome external disturbances and parametric uncertainty. These methods have demonstrated that adaptive methods can improve the robustness of the control systems.

This paper analyzes the process of the WMR's locomotion coupled with longitudinal slippage when performing skid-steering. An active feed-forward slip compensation model of time-varying slip rates is developed. We then focus on the common trajectory tracking problem and propose a new adaptive SMC method with a fast double-power reaching rate. A complete control loop for trajectory tracking is thus established. A series of simulations and experiments on the loose-soil terrain were performed to demonstrate the feasibility of the proposed control method.

The reminder of the paper is organized as follows. The common kinematic model of a skid-steered WMR is presented in Section 2. The steering locomotion process coupled with time-varying slippage is analyzed in Section 3. The new adaptive SMC law is proposed with necessary derivations, and the entire control loop is presented in Section 4. The simulation results for the WMR tracking different trajectories are shown and analyzed in Section 5. The experiment results using the proposed control method for WMR tracking trajectories in a real complex environment are shown in Section 6. Finally, the conclusion is presented in Section 7.

## 2. The Kinematic Model of the WMR

The common and simplified two-wheel kinematic model of a WMR is illustrated in Figure 1. We assume the wheels of both sides can only move longitudinally to perform skid steering. A general four-wheeled mobile robot can be deemed as sharing the same kinematic model previously mentioned when the wheels in the same side rotate in an equivalent velocity. The position of the steering center in a two-dimensional global coordinate frame is  $\mathbf{q}_c = [x_c \ y_c \ \theta_c]^T$ .

In Figure 1, the skid-steering center is marked by  $C$ . The geometric centers of the equivalent wheels on both sides are collinear with  $C$  with a spacing of  $2l$ . The diameter of the wheels is  $2r$ . Variables  $v_c$  and  $\omega_c$  are the commanded linear and angular velocity of the steering center, respectively. Variable  $\theta_c$  is the current included angle between  $v_c$  and the positive direction of  $X$  axis. The kinematic model of the WMR is then written as

$$\dot{\mathbf{q}}_c = \begin{bmatrix} \dot{x}_c \\ \dot{y}_c \\ \dot{\theta}_c \end{bmatrix} = \begin{bmatrix} \cos \theta_c & 0 \\ \sin \theta_c & 0 \\ 0 & 1 \end{bmatrix} \begin{bmatrix} v_c \\ \omega_c \end{bmatrix}. \quad (1)$$

Let  $\mathbf{q}_r = [x_r \ y_r \ \theta_r]^T$  be the desired pose of the WMR. The pose error between the current and desired poses, in the local coordinate system of the WMR, is described as

$$\mathbf{q}_e = \begin{bmatrix} x_e \\ y_e \\ \theta_e \end{bmatrix} = \begin{bmatrix} \cos \theta_c & \sin \theta_c & 0 \\ -\sin \theta_c & \cos \theta_c & 0 \\ 0 & 0 & 1 \end{bmatrix} \begin{bmatrix} x_r - x_c \\ y_r - y_c \\ \theta_r - \theta_c \end{bmatrix}. \quad (2)$$

The differential form of the pose error is therefore described as

$$\dot{\mathbf{q}}_e = \begin{bmatrix} \dot{x}_e \\ \dot{y}_e \\ \dot{\theta}_e \end{bmatrix} = \begin{bmatrix} y_e \omega_c - v_c + v_r \cos \theta_e \\ v_r \sin \theta_e - x_e \omega_c \\ \omega_r - \omega_c \end{bmatrix}. \quad (3)$$

The local coordinate frame and positive directions attached the robot body and equivalent wheels while skid-steering is as illustrated in Figure 2.  $v_l$  and  $v_r$  are the commanded linear velocities of equivalent wheels in both sides, respectively, which are parallel to  $v_c$ .  $\omega_{cl}$  and  $\omega_{cr}$  are the commanded angular velocities of the left and right equivalent wheels, with collinear rotation axes. Positive directions of linear and angular velocities are as the arrows pointing.

According to the kinematic model of the WMR, the relationship between the locomotive states of the equivalent wheels and the steering center while having slippage is

$$\begin{bmatrix} v_{sl} \\ v_{sr} \end{bmatrix} = \left[ \begin{array}{ccc|cc} 0 & 0 & -l & r & 0 \\ 0 & 0 & l & 0 & r \end{array} \right] \begin{bmatrix} \dot{\mathbf{q}}_c \\ \omega_{cl} \\ \omega_{cr} \end{bmatrix}, \quad (4)$$

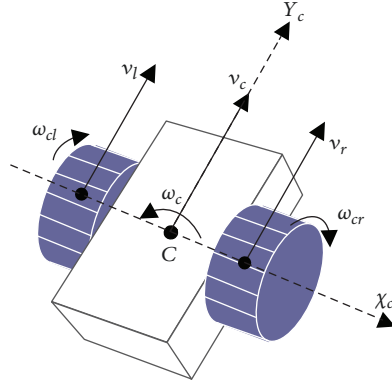


FIGURE 2: The local coordinate frame attached the robot body and wheels.

where  $v_{sl}$  and  $v_{sr}$  are the effective linear velocities of the equivalent wheels with slippage.

### 3. Active Feed-Forward Slip Compensation

Some researchers have managed to compensate for wheel slippage by predicting the probable slip rate with prior data [4, 15]. However, this approach relies on measured data in specific terrain conditions, which is not robust with respect to a changeable or unknown environment. In this paper, we consider the longitudinal slippage of a WMR as time-varying, so that online compensation is possible.

During our research on WMRs on surfaces with loose soil, we found that skids can occur when the slip rates of the two wheels are inharmonious or when the slope of the terrain is too steep. This complexity makes the skid model hard to predict and establish. On the other hand, the compensation of time-varying longitudinal slippages can be achieved by estimating the real-time slip rates of two equivalent wheels on both sides. Thus, when the effect on locomotion from the skid is weaker than that of slippage, we can compensate for the longitudinal slippage while treating skids as external bounded disturbances.

Under the condition that the internal mechanical transmission loss of a WMR is omitted, we define the slip rates of the equivalent wheels as

$$\begin{cases} s_{sl} = \frac{(v_l - v_{sl})}{v_{sl}}, \\ s_{sr} = \frac{(v_r - v_{sr})}{v_{sr}}, \end{cases} \quad (5)$$

where  $s_{sl}$  and  $s_{sr}$  are the slip rates of the left and right equivalent wheels.

According to  $v_c = 1/2(v_l + v_r)$  and  $\omega_c = (1/2l)(-v_l + v_r)$ , we can describe the actual measured kinematic state  $V_a$  of the WMR steering center as

$$V_a = \begin{bmatrix} v_a \\ \omega_a \end{bmatrix} = \mathbf{E}_s(\mathbf{q}) \begin{bmatrix} v_{sl} \\ v_{sr} \end{bmatrix} = \begin{bmatrix} v_l \\ v_r \end{bmatrix} - \mathbf{E}_s(\mathbf{q}) \begin{bmatrix} \delta_{sl} \\ \delta_{sr} \end{bmatrix}, \quad (6)$$

where

$$\mathbf{E}_s(\mathbf{q}) = \begin{bmatrix} 1 & 1 \\ \frac{1}{2} & \frac{1}{2} \\ -\frac{1}{2l} & \frac{1}{2l} \end{bmatrix}, \quad (7)$$

$\delta_{sl} = s_{sl}v_l$ , and  $\delta_{sr} = s_{sr}v_r$  are the velocity losses;  $v_a$  and  $\omega_a$  are the measured actual linear and angular velocities of the steering center.

From equation (6), we find that there are uncertain velocity losses when the slip rates are time-varying. To compensate for the loss, we differentiate both sides of equation (4) with respect to time:

$$\begin{cases} \dot{v}_{sl} = r \left[ \dot{\omega}_{cl} - \frac{1}{r} (s_{sl}\dot{v}_{sl} + \dot{s}_{sl}v_{sl}) \right], \\ \dot{v}_{sr} = r \left[ \dot{\omega}_{cr} - \frac{1}{r} (s_{sr}\dot{v}_{sr} + \dot{s}_{sr}v_{sr}) \right]. \end{cases} \quad (8)$$

We then find that

$$\dot{V}_a = \begin{bmatrix} \dot{v}_a \\ \dot{\omega}_a \end{bmatrix} = \begin{bmatrix} \dot{v}_c \\ \dot{\omega}_c \end{bmatrix} - \mathbf{M}_{s1} \begin{bmatrix} \dot{v}_a \\ \dot{\omega}_a \end{bmatrix} - \mathbf{M}_{s2} \begin{bmatrix} v_a \\ \omega_a \end{bmatrix}, \quad (9)$$

where

$$\begin{aligned} \mathbf{M}_{s1} &= \begin{bmatrix} \frac{1}{2}(s_{sl} + s_{sr}) & \frac{l}{2}(s_{sr} - s_{sl}) \\ \frac{1}{2l}(s_{sr} - s_{sl}) & \frac{1}{2}(s_{sl} + s_{sr}) \end{bmatrix}, \\ \mathbf{M}_{s2} &= \begin{bmatrix} \frac{1}{2}(\dot{s}_{sl} + \dot{s}_{sr}) & \frac{l}{2}(\dot{s}_{sr} - \dot{s}_{sl}) \\ \frac{1}{2l}(\dot{s}_{sr} - \dot{s}_{sl}) & \frac{1}{2}(\dot{s}_{sl} + \dot{s}_{sr}) \end{bmatrix}. \end{aligned} \quad (10)$$

Let  $\dot{V}_s = [\dot{v}_s \quad \dot{\omega}_s]^T = \dot{V}_c - \dot{V}_a$  be the active slip compensation control input calculated based on equation (9):

$$\dot{V}_s = \mathbf{M}_{s1} \begin{bmatrix} \dot{v}_a \\ \dot{\omega}_a \end{bmatrix} + \mathbf{M}_{s2} \begin{bmatrix} v_a \\ \omega_a \end{bmatrix}. \quad (11)$$

We can then actively compensate for the effect of the time-varying slippage of both equivalent wheels on both acceleration and velocity levels when the skid-steering of the WMR couples with the longitudinal slippage.

### 4. The Design of an Adaptive SMC Law

The slip compensation approach described above is insufficient to guarantee the performance of trajectory tracking in soft or rugged environments. Therefore, we designed a new adaptive SMC law to solve this problem.

According to the theorem in article [16]: for any  $x \in R$  and  $|x| \rightarrow \infty$ , there is  $\phi(x) = x \sin(\arctan x) \geq 0$ . The “=” holds if and only if there is  $x = 0$ .

If  $x_e = 0$ , let the Lyapunov function be

$$\dot{\mathcal{L}}_y = \frac{1}{2} y_e^2. \quad (12)$$

If  $\theta_e = -\arctan(v_r y_e)$ , there is

$$\begin{aligned} \dot{\mathcal{L}}_y &= y_e \dot{y}_e = y_e (v_a \sin \theta_e - x_e \omega_c) \\ &= -y_e x_e \omega_c - v_r y_e \sin(\arctan(v_r y_e)). \end{aligned} \quad (13)$$

Thus,  $\dot{\mathcal{L}}_y \leq 0$  holds when  $v_r y_e \sin(\arctan(v_r y_e)) \geq 0$ . It means that  $y_e$  will converge to zero when  $x_e$  converges to zero and  $\theta_e$  converges to “ $-\arctan(v_a y_e)$ ”.

Therefore, the sliding mode function is designed as

$$\dot{s} = \begin{bmatrix} \dot{s}_1 \\ \dot{s}_2 \end{bmatrix} = \begin{bmatrix} x_e \\ \theta_e + \arctan(v_a y_e) \end{bmatrix}. \quad (14)$$

We chose the double-power reaching law as in article [17]:

$$\dot{s} = -k_1 |s|^{a_1} \operatorname{sgn}(s) - k_2 |s|^{a_2} \operatorname{sgn}(s) - k_3 s, \quad (15)$$

where  $k_1, k_2, k_3 > 0$ ,  $0 < a_1 < 1$ , and  $a_2 > 1$ .

The stability of equation (15) can be proved by selecting the Lyapunov function as  $\mathcal{L}_s = 0.5s^2$ . Because there is

$$\begin{aligned} \dot{\mathcal{L}}_s &= \dot{s}\dot{s} = s(-k_1 |s|^{a_1} \operatorname{sgn}(s) - k_2 |s|^{a_2} \operatorname{sgn}(s) - k_3 s) \\ &= -k_1 |s|^{a_1+1} \operatorname{sgn}(s) - k_2 |s|^{a_2+1} \operatorname{sgn}(s) - k_3 s^2 \leq 0. \end{aligned} \quad (16)$$

According to equation (14), the sliding surface of the WMR trajectory tracking system is designed as

$$\begin{aligned} \dot{s} &= \begin{bmatrix} \dot{s}_1 \\ \dot{s}_2 \end{bmatrix} = \begin{bmatrix} -k_{11}|s_1|^{a_{11}} \operatorname{sgn}(s_1) - k_{12}|s_1|^{a_{12}} \operatorname{sgn}(s_1) - k_{13}s_1 \\ -k_{21}|s_2|^{a_{21}} \operatorname{sgn}(s_2) - k_{22}|s_2|^{a_{22}} \operatorname{sgn}(s_2) - k_{23}s_2 \end{bmatrix} \\ &= \begin{bmatrix} \dot{x}_e \\ \dot{\theta}_e + \frac{\partial \alpha}{\partial v_r} \dot{v}_r + \frac{\partial \alpha}{\partial y_e} \dot{y}_e \end{bmatrix}, \end{aligned} \quad (17)$$

where  $\frac{\partial \alpha}{\partial v_r} = y_e/(1 + (v_r y_e)^2)$ ,  $\frac{\partial \alpha}{\partial y_e} = v_r/(1 + (v_r y_e)^2)$ . This is actually a fast double-power reaching law [10].

Let the desired control input for the WMR be  $V_r = [v_r \ \omega_r]^T$  calculated based on the desired input trajectory. And the relative parameters in equations (14) and (17) can be calculated through the kinematic model in Section 2.  $V_a$  is the measured actual kinematic state of the WMR as mentioned above.  $V_c = [v_c \ \omega_c]^T$  is the commanded kinematic state from the SMC control law. The actual locomotive error based on kinematics is  $V_e = V_r - V_a$ , which satisfies  $|V_e| = [|v_e| \ |\omega_e|]^T \leq [\varepsilon_1 \ \varepsilon_2]^T$  for certain, where  $\varepsilon_1$  and  $\varepsilon_2$  are positive constant values. We use a general adaptive function  $k = \mu D(t)$  to design the adaptive control input, where  $\mu$  is the coefficient and  $D(t)$  is the positive adaptive value changing with time  $t$ .

We can thus achieve the adaptive SMC control law based on equations (3), (14), and (17):

$$\begin{bmatrix} v_c \\ \omega_c \end{bmatrix} = \begin{bmatrix} y_e \omega_c + v_r \cos \theta_e + \mu_{11} \hat{D}_1(t) |s_1|^{a_{11}} \operatorname{sgn}(s_1) + \mu_{12} \hat{D}_1(t) |s_1|^{a_{12}} \operatorname{sgn}(s_1) + k_{13}s_1 \\ \omega_r + (\partial \alpha / \partial v_r) \dot{v}_r + (\partial \alpha / \partial y_e) (v_r \sin \theta_e) + \mu_{21} \hat{D}_2(t) |s_2|^{a_{21}} \operatorname{sgn}(s_2) + \mu_{22} \hat{D}_2(t) |s_2|^{a_{22}} \operatorname{sgn}(s_2) + k_{23}s_2 \end{bmatrix} / (1 + (\partial \alpha / \partial y_e)x_e), \quad (18)$$

where  $\mu_{11}, \mu_{12}, \mu_{21}, \mu_{22} > 0$ .  $\hat{D}_1(t)$  and  $\hat{D}_2(t)$  are the expected values about bounded interferences. There must exist positive constant values satisfying  $D_1 \leq \varepsilon_1^*$  and  $D_2 \leq \varepsilon_2^*$ . They are achieved from

$$\begin{cases} \dot{\hat{D}}_1(t) = |v_e s_1|, \\ \dot{\hat{D}}_2(t) = |\omega_e s_2|. \end{cases} \quad (19)$$

The stability of the proposed adaptive SMC law in equation (18) is proved as follows. Let the Lyapunov function be

$$\mathcal{L}_v(t) = \frac{1}{2} s_1^2 + \frac{1}{2} \gamma (D \wedge_1 - \varepsilon_1^*)^2, \quad (20)$$

where  $\gamma$  is a positive constant value.

We can then derive out that

$$\begin{aligned} \dot{\mathcal{L}}_v(t) &= s_1 \dot{s}_1 + \gamma (\hat{D}_1 - \varepsilon_1^*) \dot{\hat{D}}_1 = s_1 (-\mu_{11} \hat{D}_1 |s_1|^{a_{11}} \operatorname{sgn}(s_1) \\ &\quad - \mu_{12} \hat{D}_1 |s_1|^{a_{12}} \operatorname{sgn}(s_1) - k_{13}s_1) + \gamma (\hat{D}_1 - \varepsilon_1^*) \dot{\hat{D}}_1 \\ &\leq -\mu_{11} \hat{D}_1 |s_1|^{a_{11}} |s_1| - \mu_{12} \hat{D}_1 |s_1|^{a_{12}} |s_1| \\ &\quad + \gamma (\hat{D}_1 - \varepsilon_1^*) |v_e s_1| - k_{13}s_1^2 \\ &= -\varepsilon_1^* \mu_{11} |s_1|^{a_{11}} |s_1| + (\varepsilon_1^* - \hat{D}_1) \mu_{11} |s_1|^{a_{11}} |s_1| \\ &\quad - (\varepsilon_1^* - \hat{D}_1) \gamma |v_e s_1| - \mu_{12} \hat{D}_1 |s_1|^{a_{12}} |s_1| - k_{13}s_1^2 \\ &= -\varepsilon_1^* \mu_{11} |s_1|^{a_{11}} |s_1| - \varepsilon_1^* \mu_{12} |s_1|^{a_{12}} |s_1| \\ &\quad - (\varepsilon_1^* - \hat{D}_1) (\gamma |v_e| - \mu_{11} |s_1|^{a_{11}}) |s_1| \\ &\quad - (\varepsilon_1^* - \hat{D}_1) (\gamma |v_e| - \mu_{12} |s_1|^{a_{12}}) |s_1| - k_{13}s_1^2. \end{aligned} \quad (21)$$

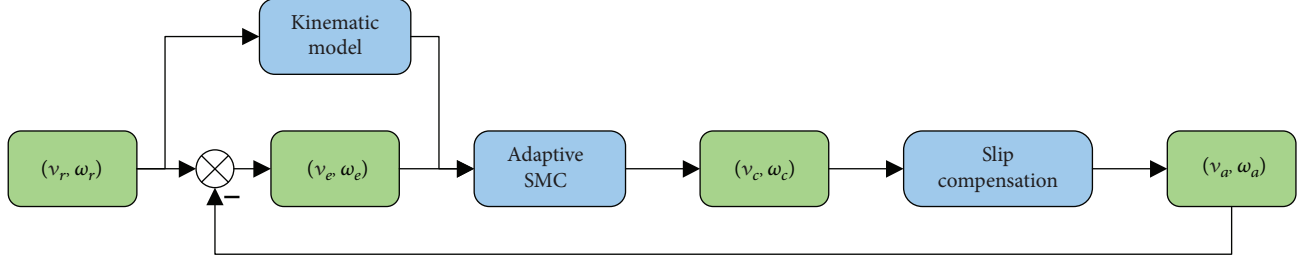


FIGURE 3: The main control loop.

The stability of equation (21) holds when  $\dot{\mathcal{L}}_v(t) \leq 0$ . This means as long as  $\gamma$  satisfies the inequalities  $\gamma > (1 + \mu_{11}|s_1|^{a_{11}})/|v_e|$  and  $\gamma > (1 + \mu_{12}|s_1|^{a_{12}})/|v_e|$ , the stability holds.

By similarly analyzing the inequality about  $s_2$ , there must exist  $\gamma$  which causes the inequality  $\gamma > \max((1 + \mu_{11}|s_1|^{a_{11}})/|v_e|, (1 + \mu_{12}|s_1|^{a_{12}})/|v_e|, (1 + \mu_{21}|s_1|^{a_{21}})/|\omega_e|, (1 + \mu_{22}|s_1|^{a_{22}})/|\omega_e|)$  to hold obviously. We can thus achieve that the system tends to be stable in finite time referring to article [18].

Since  $\dot{s}$  and  $V_e$  are uncertain and covariant with motion, the integral of  $\hat{D}(t)$  can be too large. Therefore, we set threshold conditions to prevent the adaptive parameters from accumulating too fast:

$$\begin{aligned}\dot{\hat{D}}_1(t) &= \begin{cases} |v_e s_1|, & |v_e s_1| \geq \delta_1, \\ 0, & \text{others}, \end{cases} \\ \dot{\hat{D}}_2(t) &= \begin{cases} |\omega_e s_2|, & |\omega_e s_2| \geq \delta_2, \\ 0, & \text{others}, \end{cases}\end{aligned}\quad (22)$$

where  $\delta_1$  and  $\delta_2$  are small positive values.

After the establishment of the adaptive SMC control model, the entire control loop is achieved as illustrated in Figure 3. The structure is quite straightforward and the slip compensation has been discussed in Section 3.

## 5. Simulations and Analysis

We performed simulations on whether the active slip compensation is applied as feed-forward and whether the adaptive function is applied to the SMC in MATLAB on a platform with an Intel® G4600 CPU. The units were SI in all simulations.

**5.1. Simulations on Active Slip Compensation.** The traditional SMC with a fast double-power reaching law can be achieved by substituting the parameters in equation (18) as follows:

$$\begin{cases} k_{11} = \mu_{11}\hat{D}_1(t), k_{12} = \mu_{12}\hat{D}_1(t), \\ k_{21} = \mu_{21}\hat{D}_2(t), k_{22} = \mu_{22}\hat{D}_2(t), \end{cases}\quad (23)$$

where  $k_{11}$ ,  $k_{12}$ ,  $k_{21}$ , and  $k_{22}$  are positive values. The reason we chose the traditional SMC for comparison is that we want to show how much the slip compensation alone can improve the trajectory tracking performance of SMC without the adaptive functions.

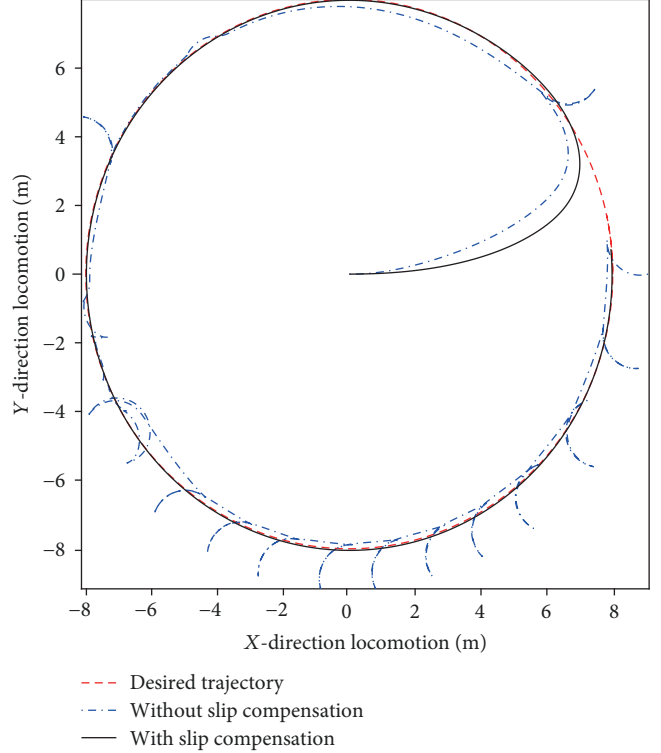


FIGURE 4: The position comparison with active slip compensation.

We assumed that the time-varying slip rates were  $s_{sl} = s_{sr} = 0.5|\sin t|$ . The interval distance between the centers of two equivalent wheels was  $l = 0.1$ , and the simulated WMR's geometric center started off from  $(0, 0)$  to follow a circular trajectory in a two-dimensional space. The commanded trajectory was described as  $x_r = 4 \cos t$ ,  $y_r = 4 \sin t$ , and  $\theta_r = t + \pi/2$ , where  $t$  is the simulation time. The parameters used for the traditional SMC law were

$$\begin{cases} k_{11} = k_{12} = k_{21} = k_{22} = 1, k_{13} = k_{23} = 5, \\ a_{11} = a_{21} = 2, a_{12} = a_{22} = 0.5. \end{cases}\quad (24)$$

The simulation results for the WMR's motion while tracking the commanded circular trajectory are shown in Figure 4. The results for errors in the  $X$ -direction, the  $Y$ -direction, and the steering angle are shown in Figures 5–7, respectively. The comparison of absolute error ratios for tracking the circular trajectory is shown in Table 1. The absolute error ratio is calculated from the accumulated simulation

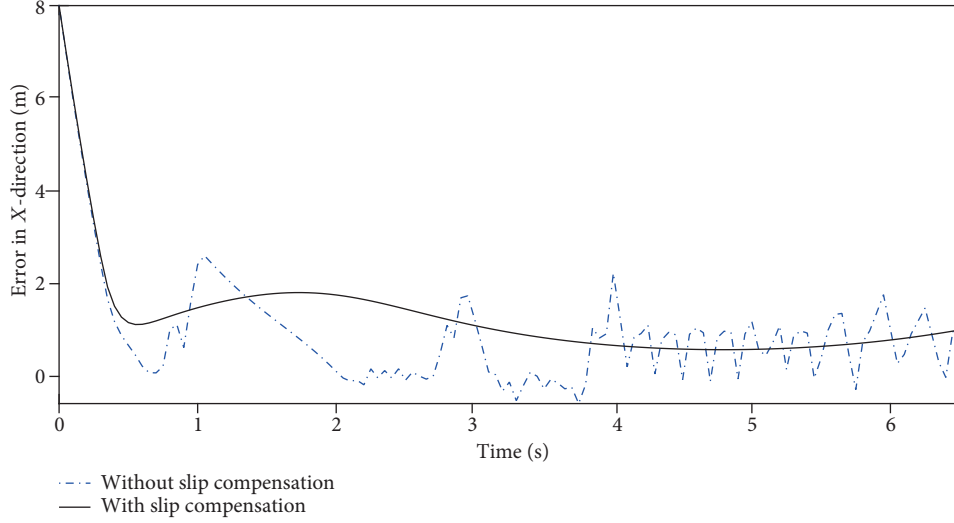


FIGURE 5: The comparison of error in the X-direction with active slip compensation.

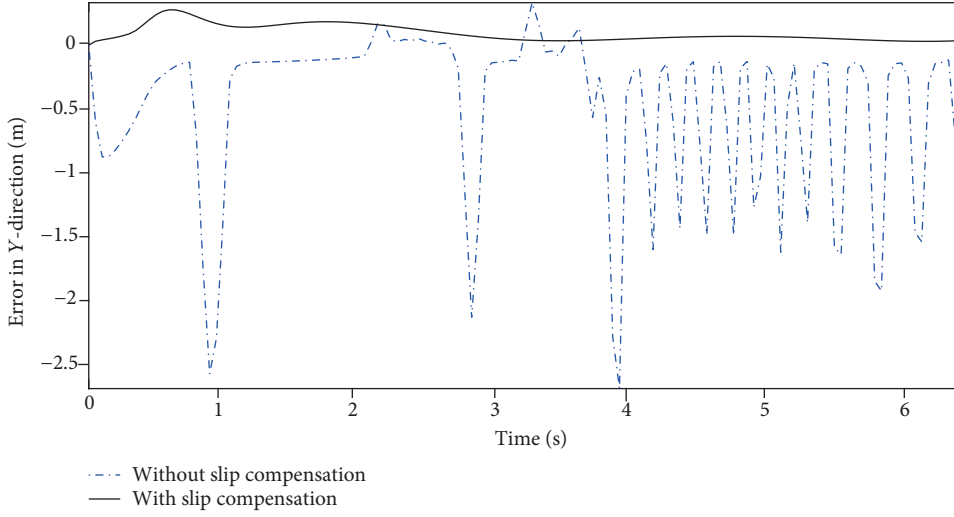


FIGURE 6: The comparison of error in the Y-direction with active slip compensation.

error divided by the accumulated desired output. The lower the absolute error ratio is, the better the capability of instantaneous responding is for that method.

When the slippage is time-varying and bounded, the traditional SMC law cannot promise steady tracking of a desired trajectory. On the other hand, trajectory tracking is obviously stable while applying slip compensation. Although active slip compensation leads to a higher error ratio in the X-direction, it still promises lower error ratios in the Y-direction and the steering angle. The output chattering caused by external uncertainty is significantly suppressed. It means that the feed-forward control path we design is necessary for a WMR tracking trajectories in uncertain environments with wheel slippage.

**5.2. Simulations of the Adaptive SMC.** To show how the adaptive function affects the SMC performance, we designed a cosine curve as the target trajectory for a more complex simulation. The time-varying slip rates were set to  $s_{sl} = s_{sr} = 0.5 |\sin t|$ .

We assumed the WMR's geometric center started from  $(0, 0)$  and tracked the cosine trajectory described by  $x_r = t$ ,  $y_r = 2 \cos(t/3 + \pi/6)$ , and  $\theta_r \in [-\pi, \pi]$ , where  $t$  is the simulation time. The parameters of the traditional SMC were the same as in the previous section. The adaptive SMC parameters were similarly set as

$$\begin{cases} \mu_{11} = \mu_{12} = \mu_{21} = \mu_{22} = 0.001, k_{13} = k_{23} = 5, \\ a_{11} = a_{21} = 2, a_{12} = a_{22} = 0.5, \\ \delta_1 = \delta_2 = 0.01. \end{cases} \quad (25)$$

Both methods used for comparison were implemented by adding the active slip feed-forward. The simulation result for position changes while tracking the cosine trajectory in a two-dimensional space is shown in Figure 8. The comparisons for errors in the X-direction, the Y-direction, and the steering angle are shown in Figures 9–11, respectively.

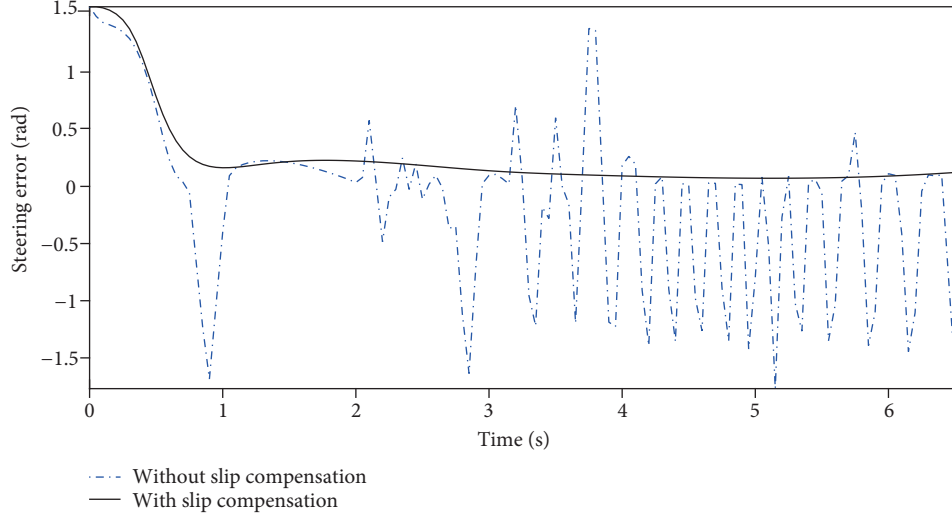


FIGURE 7: The comparison of error in the steering angle with active slip compensation.

TABLE 1: The comparison of the accumulated absolute error ratios while tracking a circular trajectory.

	X-direction	Y-direction	Steering angle
Without slip feed-forward	18.538%	10.159%	10.911%
With slip feed-forward	24.428%	1.19%	4.951%

The value changes of the adaptive functions are shown in Figure 12. Thus, we have shown that the chattering of the traditional SMC has been significantly suppressed by the adaptive function along the tracking process except around the first sharp turn. This is because the robustness is weak when the adaptive parameters are initially adjusting themselves. But once the adaptive adjustment is nearly finished, the robustness will be obviously better than methods without adaptive control.

The comparison of accumulated absolute error ratios for the cosine trajectory tracking is shown in Table 2. The accumulating error of the steering angle is quite large with both methods, because the steering angle constantly adjusts to the cosine curve and needs to turn sharply. The overall error of the adaptive SMC is slightly higher than that of the traditional SMC. This is because the adaptive adjustment of parameters can delay the response speed, resulting in higher error ratios in the system. The traditional SMC usually responds faster to the desired trajectory changing but has obviously more chattering. Therefore, the adaptive SMC is suitable for tracking missions putting priority to steadiness and smoothness, instead of the capability of instantaneous response. This feature makes our method appropriate for the trajectory tracking missions as mentioned in Section 1.

The chattering usually occurs during the starting period and rapid steering angle changing. From the simulations described above, we can conclude that both the active slip feed-forward and the adaptive control functions can signif-

icantly suppress the chattering of the system, without sacrificing much performance in simulations. The external interferences caused by slip loss and unpredictable errors were greatly suppressed. These improvements are important not only for simulations but also for practical usage. This is because the actual disturbances to a WMR in a real and complex environment are usually more unpredictable, which will be discussed in the following section.

## 6. Experiments and Analysis

To demonstrate the improvement to the performance of trajectory tracking by implementing the active slip compensation and the adaptive SMC, we performed a series of experiments with a WMR on loose soil. It carried a Raspberry Pi mounted by the ROS (Robot Operating System). The real-time actual pose of the WMR was measured by the OptiTrack visual measurement system. The experiment scene is shown in Figure 13. The units were SI in all experiments.

We performed cosine trajectory tracking experiments with four different methods. They were open-loop experiments with and without active slip compensation and closed-loop experiments using SMC with and without adaptive control. The control frequency was 17 Hz for all methods.

With the units being SI, the desired cosine trajectory was as  $x_r = \pi t / 60$ ,  $y_r = 0.4 \cos(3.5x_r) - 0.4$ , and  $\theta_r \in [-\pi, \pi]$ , where  $t$  is the running time. The desired velocities were calculated using position and angular differentiation. The parameters for the traditional SMC and the adaptive SMC were set as

$$\begin{cases} k_{11} = k_{12} = 0.005, k_{21} = k_{22} = 0.1, \\ \mu_{11} = \mu_{12} = 0.001, \mu_{21} = \mu_{22} = 0.004, \\ k_{13} = 0.01, k_{23} = 1, \\ a_{11} = 0.05, a_{21} = 0.1, a_{12} = 1.5, a_{22} = 2, \\ \delta_1 = \delta_2 = 0.001. \end{cases} \quad (26)$$

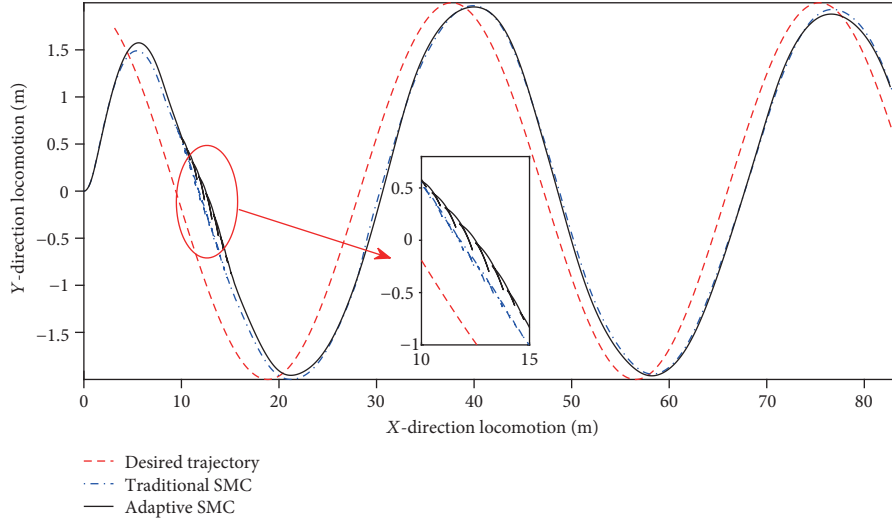


FIGURE 8: The comparisons of position changes with SMCs.

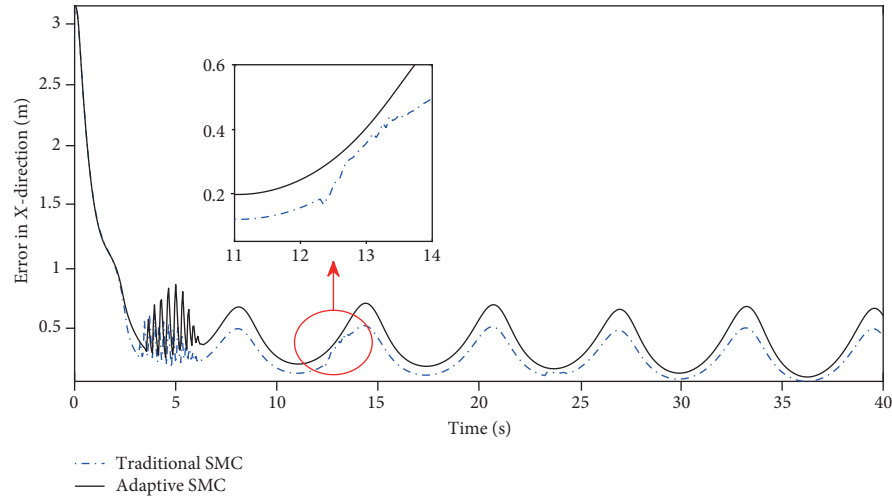


FIGURE 9: The comparison of errors in X-direction with SMCs.

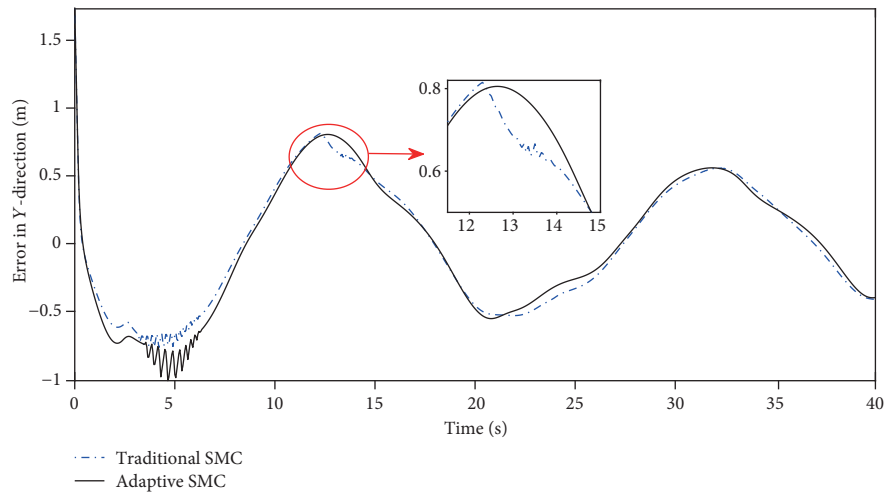


FIGURE 10: The comparison of errors in Y-direction with SMCs.

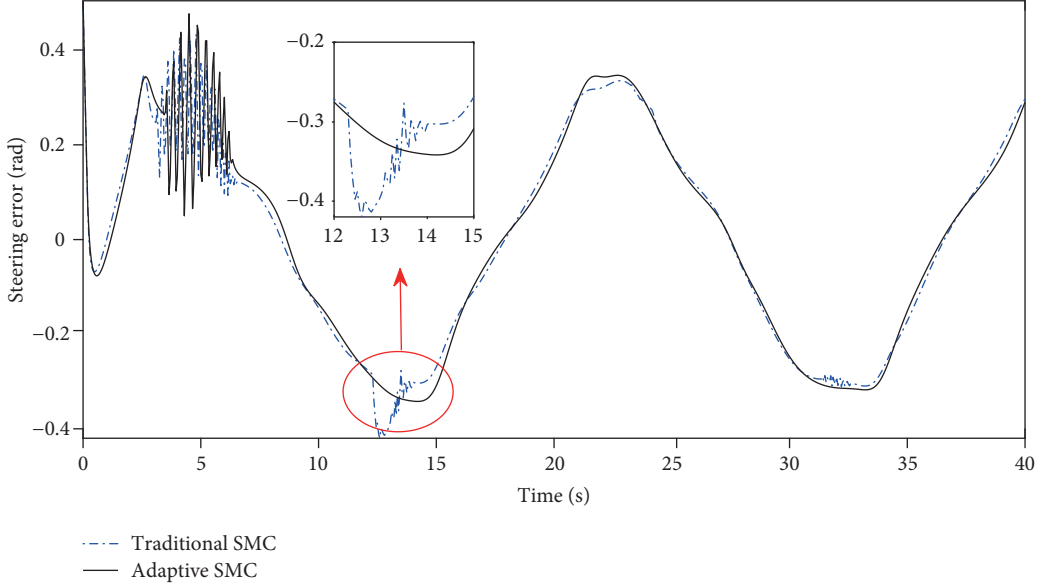


FIGURE 11: The comparison of errors in steering angle with SMCs.

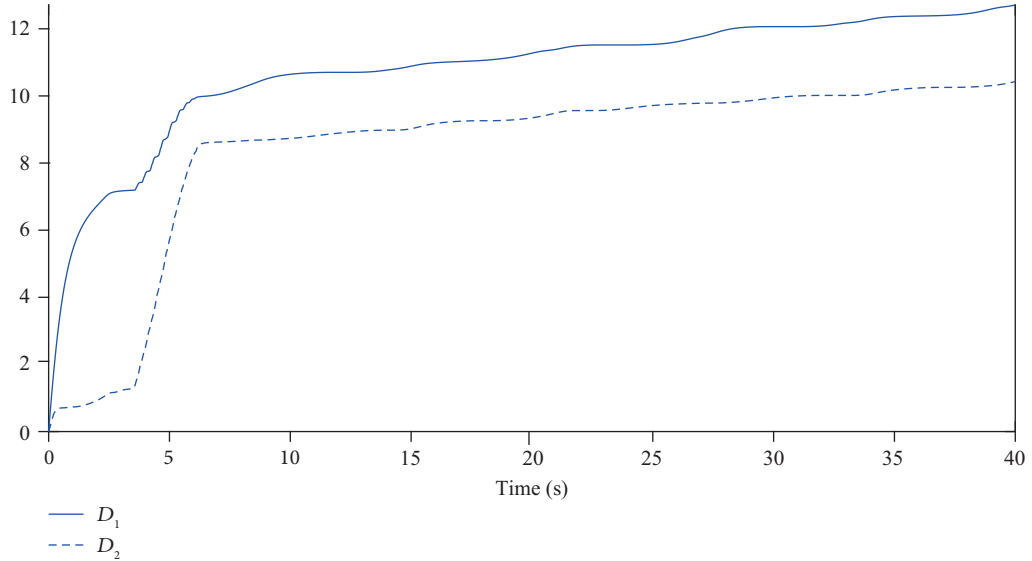


FIGURE 12: The value changes of the adaptive functions.

The experiment results of the WMR's positions on loose soil are shown in Figure 14. The experiment results of errors in the X-direction, the Y-direction, and the steering angle are shown in Figures 15–17, respectively. The value changes of the adaptive functions are shown in Figure 18. The slip rate changes of the WMR are shown in Figure 19. When the damping of the system is unpredictable, such as in our experiments where the WMR locomotes on loose soil, the chattering can obviously affect the overall trajectory tracking performance. The undulation of actual longitudinal slippage with the adaptive SMC was less severe than with traditional SMC as shown in the results.

The comparison of absolute error ratios of tracking the cosine trajectory with these different control methods is shown in Table 3. Although the traditional SMC can have

TABLE 2: The comparison of accumulated absolute error ratios from SMC tracking a cosine trajectory.

	X-direction	Y-direction	Steering angle
Traditional SMC	2.35%	23.866%	342.25%
Adaptive SMC	2.524%	24.387%	342.07%

lower error ratios according to the simulation results in the previous section, its lacking capability of suppressing the occurrence of chattering results in relatively worse tracking performance in our experiments. The adaptive SMC outperforms the other methods in all respects we are interested in.

It also should be mentioned that both the SMC methods failed when there was no slip feed-forward path



FIGURE 13: The experiment scene.

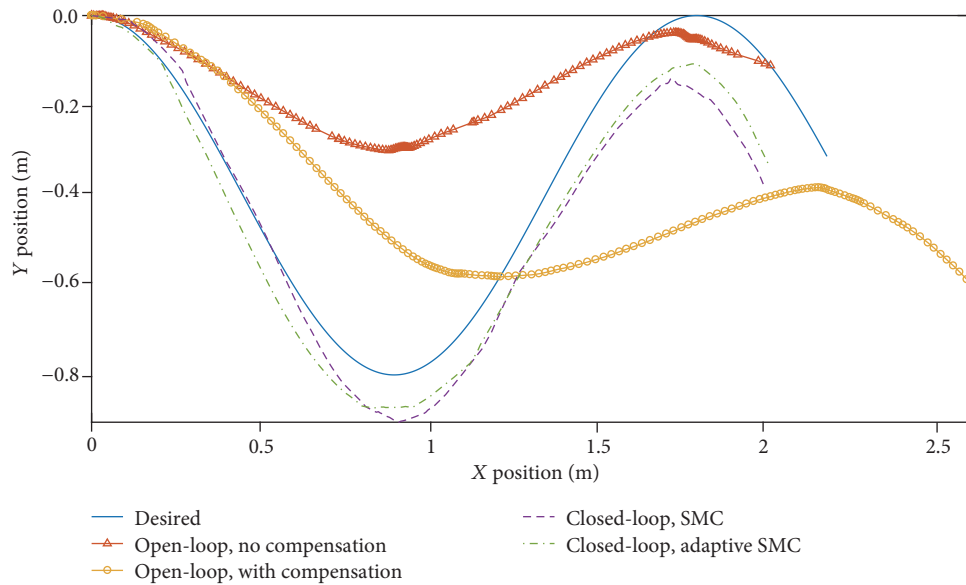


FIGURE 14: The comparison of position changes.

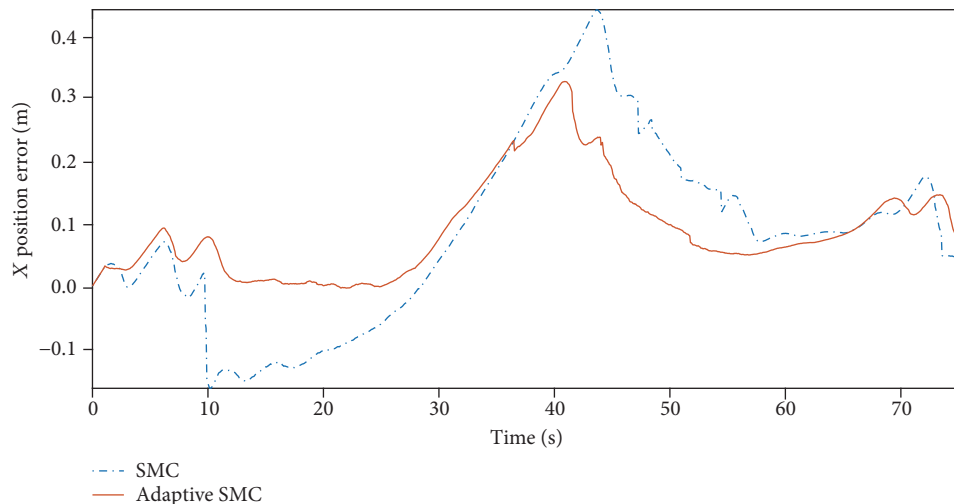


FIGURE 15: The comparison of errors in X-direction with SMCs.

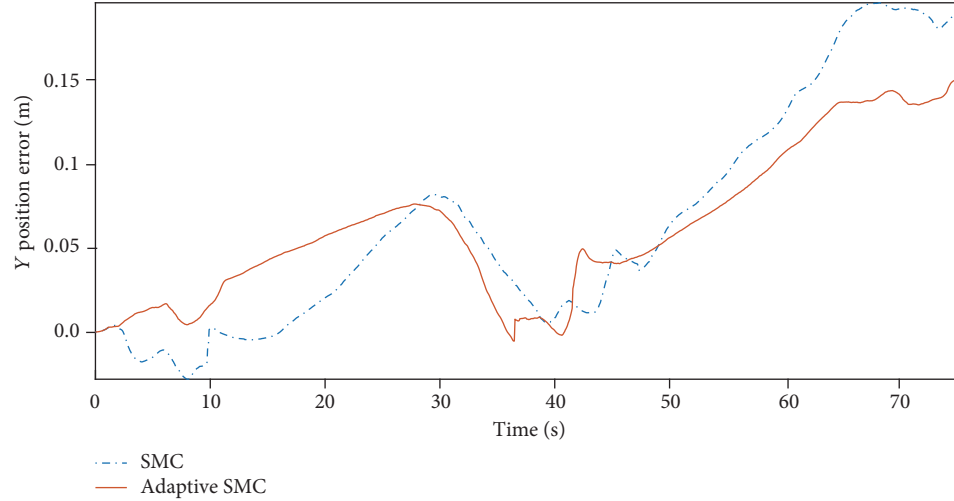


FIGURE 16: The comparison of errors in Y-direction with SMCs.

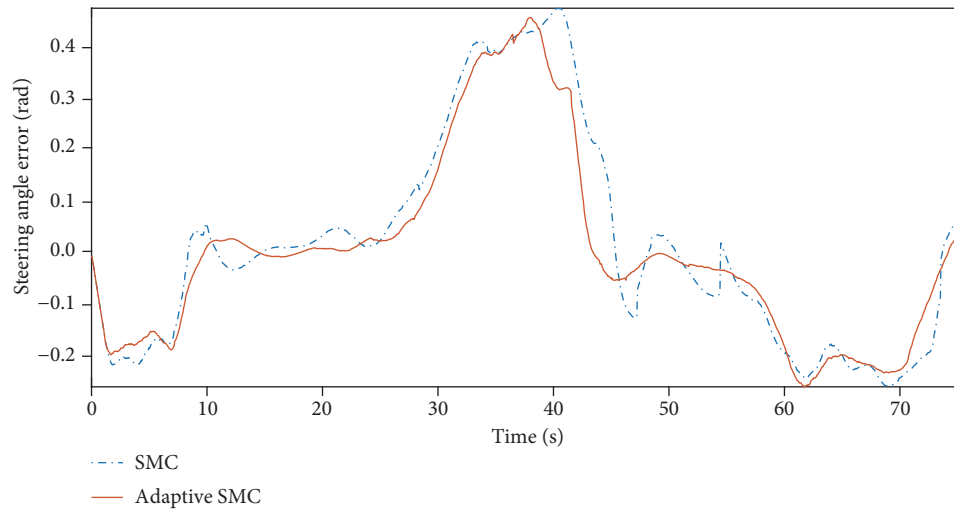


FIGURE 17: The comparison of steering angle with SMCs.

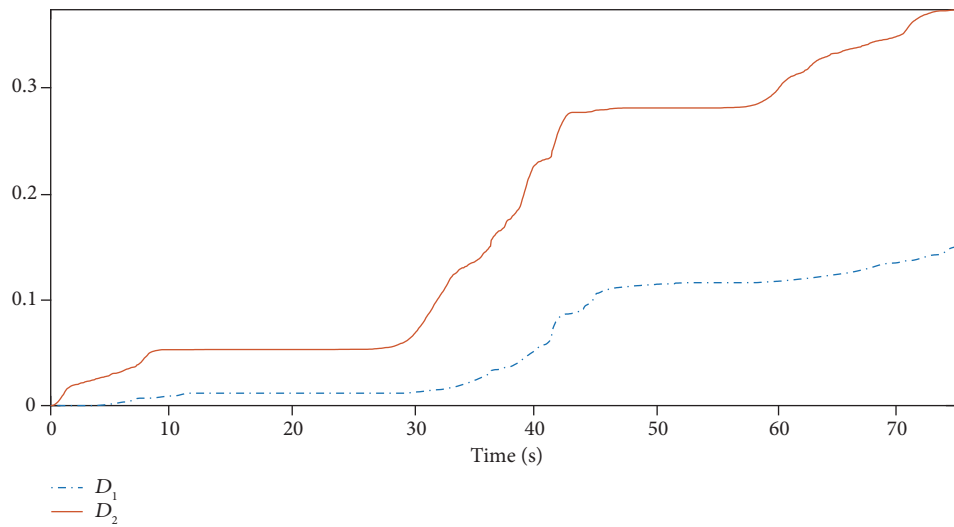


FIGURE 18: The value changes of the adaptive functions with SMCs.

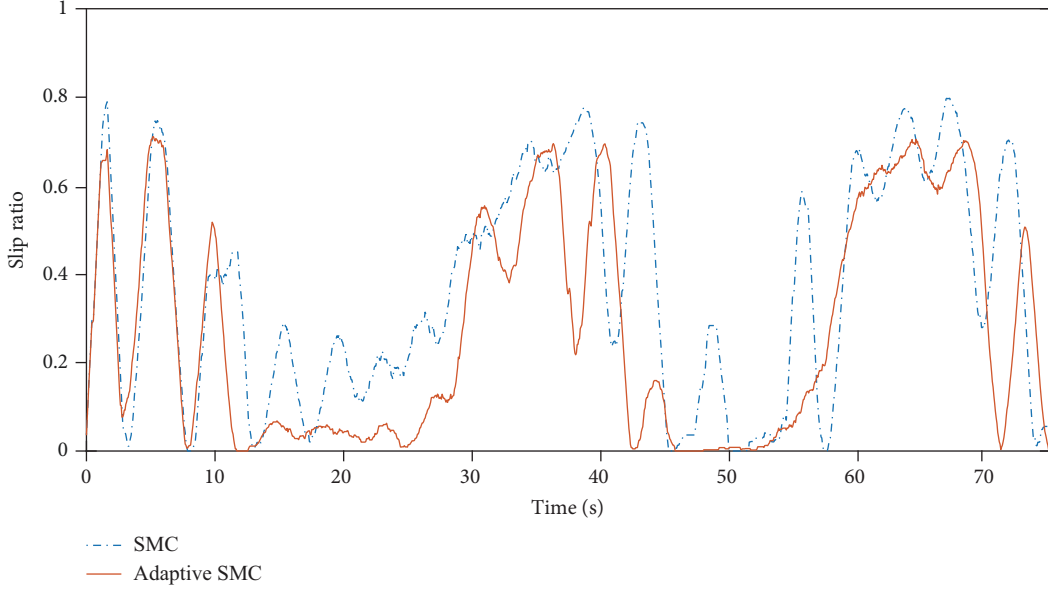


FIGURE 19: The slip rate changes of the WMR with SMCs.

TABLE 3: The comparison of accumulated absolute error ratios with different control methods for tracking a cosine trajectory.

	X-direction	Y-direction	Steering angle
Open-loop, without slip compensation	13.082%	46.608%	62.828%
Open-loop, with slip compensation	14.427%	60.566%	55.195%
Traditional SMC with slip compensation	10.59%	22.425%	20.799%
Adaptive SMC with slip compensation	7.457%	19.612%	17.558%

and thus are not shown in the comparisons. The WMR lacking slip compensation gets stuck in spinning, which indicates that this feed-forward can be indispensable in a real complex environment.

## 7. Conclusion

In this paper, we described an active slip feed-forward compensation for the WMR control system based on the time-varying longitudinal slippage, which makes the trajectory tracking mission in complex environments such as on loose soil viable with the general WMRs. We proposed a new adaptive SMC with a fast double-power reaching law for the WMR to effectively track commanded trajectories. By combining the adaptive SMC with the slip feed-forward, the chattering of the WMR's trajectory has been significantly suppressed. However, in our simulation, this results in slightly higher error rates than using the traditional SMC approach. To demonstrate the feasibility of the proposed method in complex environments, we conducted a series of trajectory tracking experiments on loose-soil terrain with our WMR using a ROS. The experimental results show that by reducing the chattering caused by the wheel-soil slippage and the control law, the tracking errors were significantly decreased. The method proposed in this paper outperforms all other competitors under similar experiment conditions in all respects we are interested in.

Although there were some positive results in the simulations and experiments, we found that the tracking errors are still not negligible during real-world experiments. The main reason is that sharp turns on soft terrain exceeded the mechanical capability of our WMR, resulting in wheels sinking into loose soil at some moments. This means that the current control scheme of continuously pushing the WMR forward should be improved in our further research for a better trajectory tracking performance.

## Data Availability

The data used to support the findings of this study are available from the corresponding author upon request. Our SMC toolbox has been open-sourced in <https://github.com/orcasdli/SMCinROS>.

## Conflicts of Interest

The author(s) declare(s) that they have no conflicts of interest.

## Acknowledgments

This study was supported by the National Natural Science Foundation of China (Grant No. 51822502) and the National Basic Research Program of China (Grant No. 2013CB035502).

## Supplementary Materials

The experiment video shows the experiment of using the WMR to track a cosine trajectory with 4 different methods as mentioned in Section 6 of the manuscript. (*Supplementary Materials*)

## References

- [1] H. Shibly, K. Iagnemma, and S. Dubowsky, “An equivalent soil mechanics formulation for rigid wheels in deformable terrain, with application to planetary exploration rovers,” *Journal of Terramechanics*, vol. 42, no. 1, pp. 1–13, 2005.
- [2] L. Ding, H. Gao, Z. Deng, K. Yoshida, and K. Nagatani, “Slip ratio for lugged wheel of planetary rover in deformable soil: definition and estimation,” in *2009 IEEE/RSJ International Conference on Intelligent Robots and Systems*, pp. 3343–3348, St. Louis, MO, USA, October 2009.
- [3] L. Ding, J. Guo, B. Yan et al., “Longitudinal skid experimental investigation for wheels of planetary exploration rovers,” *Journal of Mechanical Engineering*, vol. 51, no. 18, pp. 99–107, 2015.
- [4] D. Liang, G. Haibo, G. Junlong, L. Nan, D. Guangren, and L. Ximin, “Terramechanics-based analysis of slipping and skidding for wheeled mobile robots,” in *Proceedings of the 31st Chinese Control Conference*, pp. 4966–4973, Hefei, China, 2012.
- [5] M. Partovibakhsh and G. Liu, “Slip ratio estimation and control of wheeled mobile robot on different terrains,” in *2015 IEEE International Conference on Cyber Technology in Automation, Control, and Intelligent Systems (CYBER)*, pp. 566–571, Shenyang, China, 2015.
- [6] T. Fukao, H. Nakagawa, and N. Adachi, “Adaptive tracking control of a nonholonomic mobile robot,” *IEEE Transactions on Robotics and Automation*, vol. 16, no. 5, pp. 609–615, 2000.
- [7] I. Matraji, A. al-Durra, A. Haryono, K. al-Wahedi, and M. Abou-Khousa, “Trajectory tracking control of skid-steered mobile robot based on adaptive second order sliding mode control,” *Control Engineering Practice*, vol. 72, pp. 167–176, 2018.
- [8] A. Mehta and B. Bandyopadhyay, “Frequency-shaped and observer-based discrete-time sliding mode control,” in *SpringerBriefs in Applied Sciences and Technology*, pp. 9–25, Springer, 2015.
- [9] W.-F. Xie, “Sliding-mode-observer-based adaptive control for servo actuator with friction,” *IEEE Transactions on Industrial Electronics*, vol. 54, no. 3, pp. 1517–1527, 2007.
- [10] H. X. Zhang, J. S. Fan, F. Meng, and J. F. Huang, “A new double power reaching law for sliding mode control,” *Control and Decision*, vol. 28, no. 2, pp. 289–293, 2013.
- [11] C. Gu, J. Jiang, and Y. Wu, “Tracking control for a near-space vehicle in the ascent phase,” *Journal of Harbin Engineering University*, vol. 37, no. 11, pp. 1526–1531, 2016.
- [12] K. Liu, Y. Cao, S. Wang, and Y. Li, “Terminal sliding mode control for landing on asteroids based on double power reaching law,” in *2015 IEEE International Conference on Information and Automation*, pp. 2444–2449, Lijiang, China, 2015.
- [13] V. T. Yen, W. Y. Nan, P. van Cuong, N. X. Quynh, and V. H. Thich, “Robust adaptive sliding mode control for industrial robot manipulator using fuzzy wavelet neural networks,” *International Journal of Control, Automation and Systems*, vol. 15, no. 6, pp. 2930–2941, 2017.
- [14] H. Wang, X. Zhao, and Y. Tian, “Trajectory tracking control of XY table using sliding mode adaptive control based on fast double power reaching law,” *Asian Journal of Control*, vol. 18, no. 6, pp. 2263–2271, 2016.
- [15] L. Ding, S. Li, Y. J. Liu, H. Gao, C. Chen, and Z. Deng, “Adaptive neural network-based tracking control for full-state constrained wheeled mobile robotic system,” *IEEE Transactions on Systems, Man, and Cybernetics: Systems*, vol. 47, no. 8, pp. 2410–2419, 2017.
- [16] M. Gianni, F. Ferri, M. Menna, and F. Pirri, “Adaptive robust three-dimensional trajectory tracking for actively articulated tracked vehicles\*,” *Journal of Field Robotics*, vol. 33, no. 7, pp. 901–930, 2016.
- [17] W. Wu, H. Chen, and Y. Wang, “Global trajectory tracking control of mobile robots,” *Acta Automatica Sinica*, vol. 27, no. 3, pp. 326–331, 2001.
- [18] F. Plestan, Y. Shtessel, V. Brégeault, and A. Poznyak, “New methodologies for adaptive sliding mode control,” *International Journal of Control*, vol. 83, no. 9, pp. 1907–1919, 2010.

